EXIT Chart Aided Design of DS-CDMA UltraWideBand Systems Using Iterative Decoding

R. A. Riaz, M. El-Hajjar, Q. Z. Ahmed, S. X. Ng, S. Chen and L. Hanzo
School of Electronics and Computer Science, University of Southampton, SO17 1BJ, UK.
Email: {rar06r,meh05r,qza05r,sxn,sqc,lh}@ecs.soton.ac.uk,
http://www-mobile.ecs.soton.ac.uk

***Abstract*— This paper presents a novel UltraWideBand (UWB), Direct Sequence Code Division Multiple Access (DS-CDMA) aided system designed for the IEEE 802.15.3a UWB channel specifications. Substantial performance improvements can be attained by serially concatenated channel encoding combined with a Unity Rate Code (URC). We compare the performance of the iterative aided decoding Correlation (Corr) and Minimum Mean Square Error (MMSE) detectors exchanging extrinsic information between the URC's decoder as well as the outer Recursive Systematic Convolutional (RSC) code's decoder. Moreover, the iterative decoding convergence analysis of the proposed system is carried out with the aid of Extrinsic Information Transfer (EXIT) charts. As expected, the iteratively decoded fully-loaded system employing MMSE detection outperforms its counterpart employing the equivalent Corr detection. Explicitly, UWB DS-CDMA using the MMSE detector attains a BER of 10^{-5} at $\frac{E_b}{N_o} = 2dB$ when supporting $U = 32$ users employing $i = 12$ decoding iterations, while the same system using the Corr detector operates at BER-10^{-1}.**

I. Introduction

Recently, UltraWideBand (UWB) systems have attracted substantial interest in the research community. Their high bandwidth results in a fine time domain received signal resolution, leading to accurate position sensing. Furthermore, owing to its wide bandwidth, the received UWB signal is constituted by a high number of multipath components [1]. The Federal Communications Commission's (FCC) ruling released the band spanning from 3.1 to 10.6 GHz in the USA for UWB [2]. In [3], UWB communications were proposed for both Wireless Sensor Networks (WSN) and Personal Area Networks (PAN). Furthermore, the IEEE 802.15.3a standardazition task group has ratified a standardrized channel model to be used for the evaluation of PAN physical layer protocols [4].

Several authors [5] have considered the iterative decoding of diverse spectrally efficient modulation schemes. In [6], the turbo principle was used for iterative soft demapping in the context of multilevel modulation schemes combined with channel decoding. In [7], Unity Rate Codes (URC) were used for designing low complexity turbo codes suitable for both bandwidth and power-limited systems having stringent Bit Error Rate (BER) requirements.

The Extrinsic Information Transfer (EXIT) chart concept was proposed by ten Brink [8] as a tool designed for analysing the convergence behaviour of iteratively decoded systems. EXIT charts are capable of predicting the SNR value required for achieving an infinitesimally low BER after a sufficiently high number of detection iterations. In this contribution, we analyse the convergence performance of an iteratively decoded UWB DS-CDMA system employing two different decoders, an iterative Correlation (Corr) receiver and that of a Minimum Mean Square Error (MMSE) receiver using EXIT charts.

The novelty and rationale of the proposed system can be summarised as follows:

1) *We investigate an iterative detection aided DS-CDMA UWB system capable of resolving a high number of received signal components for the sake of increasing the achievable diversity gain.*
2) *Iterative detection exchanging extrinsic information between the inner URC's decoder and the outer convolutional code's decoder is employed and analysed using EXIT charts. The URC is capable of completely eliminating the system's error-floor as well as facilitating operation at the lowest possible turbo-cliff SNR without significantly increasing the associated complexity or interleaver delay.*

The rest of this paper is organised as follows. In Section II we introduce our system model, followed by Section III, where the UWB transmitter and receiver are detailed. Our results are discussed in Section IV, followed by our conclusions and future research ideas in Section V.

II. System Model

Figure 1 shows the discrete-time baseband model of the iteratively detected DS-CDMA UWB system. Each user transmits a data symbol sequence $\mathbf{m}^{(u)}$ consisting of N elements at symbol intervals T_s. Each data symbol $\mathbf{m}_n^{(u)}$ of user u is repeated S times and the resultant S-dimensional vector is multiplied by the S chips of the specific signature sequence $\mathbf{s}^{(u)}$, having a period of S. Each of the U channels is described by the UWB Channel Impulse Response (CIR) $\mathbf{h}^{(u)}$ consisting of W samples during the chip interval $T_c = \frac{T_s}{S}$. As shown in Figure 1, the received complex-valued symbols are first detected by the Corr or MMSE detector in order to produce the corresponding estimated data bits $\hat{\mathbf{m}}$, which are fed into the BPSK softbit demodulator which calculates the log-likelihood ratio (LLR) based on the Log Maximum Aposteriori Probability (Log-MAP) algorithm [9]. As seen in Figure 1, the URC decoder processes the information forwarded to it by the BPSK softbit demodulator in conjunction with the $a\ priori$

The financial support of the COMSATS Institute of Information Technology under the auspices of Higher Education Commission, Pakistan, and that of the EPSRC, UK, is gratefully acknowledged.

978-1-4244-1722-3/08/$25.00 ©2008 IEEE.

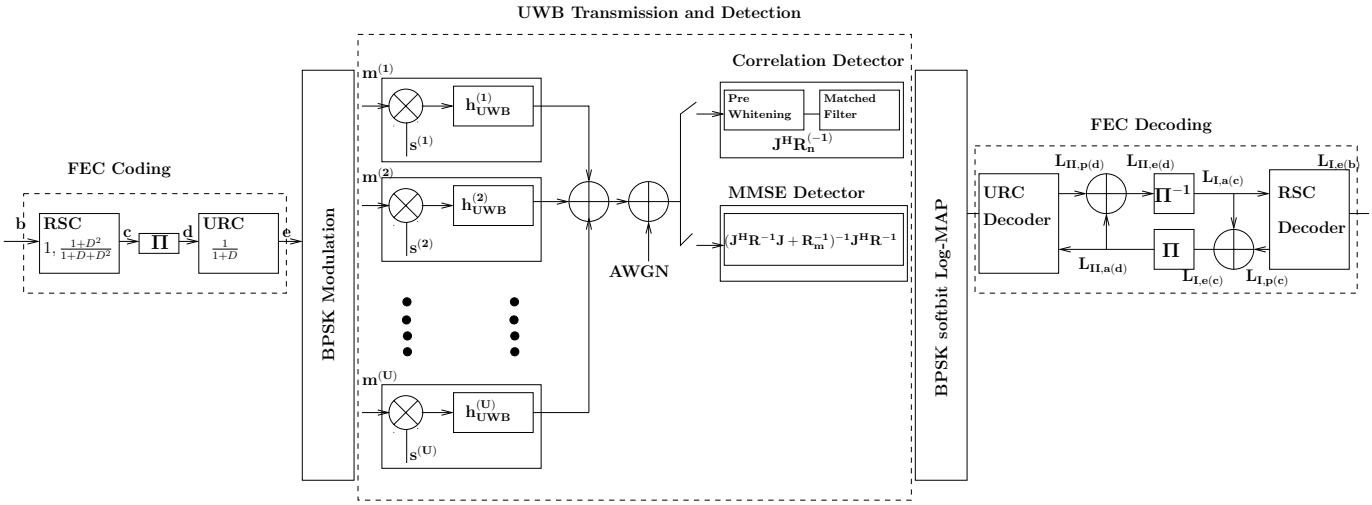

Fig. 1. The proposed Discrete-time baseband UWB iteratively decoded system model.

information in order to generate the $a\ posteriori$ probability. The $a\ priori$ Log-Likelihood Ratio (LLR) values output by the URC decoder are subtracted from the $a\ posteriori$ LLR values provided by the log-MAP algorithm, for the sake of generating the extrinsic LLR values $L_{II,e(d)}$, as seen in Figure 1. Next, the soft bits $L_{I,a(c)}$ are passed to the convolutional decoder of Figure 1 in order to compute the $a\ posteriori$ LLR values $L_{I,p(c)}$ provided by the Log-MAP algorithm for all the channel-coded bits. During the last iteration only the LLR values $L_{I,e(b)}$ of the original uncoded systematic information bits are required, which are passed to the hard decision based Recursive Systematic Convolutional (RSC) decoder in order to determine the estimated transmitted source bits. As seen in Figure 1, the extrinsic information $L_{I,e(c)}$ is generated by subtracting the $a\ priori$ information from the $a\ posteriori$ information according to $\left[(L_{I,p(c)} - L_{I,a(c)})\right]$, which is then fed back to the URC decoder as the $a\ priori$ information $L_{II,a(d)}$ after appropriately reordering them using the interleaver of Figure 1.

III. UWB Transmission and Detection

A. DS-UWB Baseband Signal

In direct sequence UWB systems, which are analogous to conventional direct sequence spread spectrum (DS-SS) systems [10], the signalling pulse transmissions are controlled by a pseudo random noise code, obeying an appropriate finite bandwidth chip waveform generating an UWB signal. The v^{th} data bit of user u can be transmitted using binary pulse amplitude modulation (BPAM) and the transmitted signal $g^{(u)}(t)$ is formulated as:

$$g^{(u)}(t) = \sum_{v=0}^{\infty} \sum_{q=0}^{S-1} \psi(t - vT_s - qT_c) s_q^{(u)} m_v^{(u)}, \qquad (1)$$

where $\psi(t)$ is the chip waveform representing the UWB pulse, which controls the bandwidth of the UWB signal, $m_v^{(u)}$ corresponds to the data information of user u, T_c is the chip duration and $s_q^{(u)}$ is the q^{th} chip of the spreading code of user u. We assume that a block of data consisting of M bits is transmitted within the block duration of $0 < t \leq MT_b = T_s$, where T_b is the bit duration. The DS-SS waveform $s^{(u)}(t)$ of user u consists of a periodic Pseudo Noise (PN) sequence having a length of S chips, which can be expressed as $s^{(u)}(t) = \sum_{q=0}^{S-1} s_q^{(u)} \psi(t - qT_c)$, where $s_q^{(u)}$ assumes a value of +1 or -1.

B. Channel Model

The complex valued low-pass multipath CIR can be expressed as [11, 12]

$$h(t) = \sum_{x=0}^{\infty} \sum_{z=0}^{\infty} \alpha_{zx} e^{j\phi_{zx}} \delta(t - T_x - \tau_{zx}), \qquad (2)$$

where the gain of the z^{th} ray of the x^{th} cluster is α_{zx} and its phase is ϕ_{zx}, while T_x is the x^{th} cluster's arrival time and τ_{zx} is the z^{th} ray of the x^{th} cluster's arrival time. Furthermore, ϕ_{zx} represents a statistically independent uniformly distributed random variable spanning over $[0, 2\pi)$ and α_{zx} is a statistically independent positive random variable having a Rayleigh probability density function (PDF) given by $p(\alpha_{zx}) = (\frac{2\alpha_{zx}}{\overline{\alpha_{zx}^2}}) e^{(\frac{-\alpha_{zx}^2}{\overline{\alpha_{zx}^2}})}$. The mean square values $\overline{\alpha_{zx}^2}$ are monotonically decreasing functions of T_x and τ_{zx} given by $\overline{\alpha_{zx}^2} = \overline{\alpha^2(T_x, \tau_{zx})} = \overline{\alpha^2(0,0)} e^{\frac{-T_x}{\Gamma}} e^{\frac{-\tau_{zx}}{\gamma}}$, where $\overline{\alpha^2(0,0)}$ = $\overline{\alpha_{00}^2}$ is the average power gain of the first ray of the first cluster. Furhermore, the variables Γ and γ represent the power decay time constants for the clusters and rays respectively, as potrayed in the stylized model of Figure 2.

C. Receiver Model

The composite transmitted data sequence of the U users can be written as $\mathbf{m} = \left[\mathbf{m}^{(1)T}, \mathbf{m}^{(2)T}, ..., \mathbf{m}^{(U)T}\right]^T$, where $m_j = m_n^{(u)}$ for $j = n + N(u-1)$, $u = 1, 2, ..., U$ and

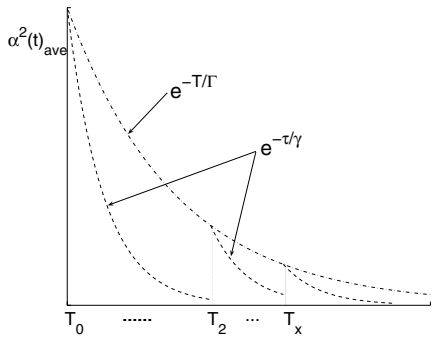

Fig. 2. Stylized UWB CIR.

$n = 1, 2...., N$. The overall system matrix $\mathbf{J}$ can be interpreted as

$$[\mathbf{J}]_{ij} = \begin{cases} b_n^{(u)}(l) & \text{for } u = 1, 2, ..., U;\ n = 1, 2, ..., N \\ & l = 1, 2, ..., S + W - 1 \\ 0 & \text{otherwise,} \end{cases} \quad (3)$$

where $i = 1, ..., NS + W - 1,\ j = 1, ..., UN$. The structure of the system matrix considered is highlighted in Figure 3. In Equation (3) the combined impulse response, $\mathbf{b}_n^{(u)}$ is given by:

$$\begin{aligned} \mathbf{b}_n^{(u)} &= \left[b_n^{(u)}(1), b_n^{(u)}(2), ..., b_n^{(u)}(l), ..., b_n^{(u)}(S + W - 1)\right]^T \\ &= \mathbf{s}^{(u)} * \mathbf{h}_n^{(u)}, \end{aligned} \quad (4)$$

where $u = 1, 2, ..., U,\ n = 1, 2...., N,\ l = 1, 2, ..., S + W - 1$. Furthermore, $\mathbf{s}^{(u)}$ and $\mathbf{h}_n^{(u)}$ are the corresponding S-chip spreading sequence vector and the W-chip CIR vector encountered at the chip rate of $\frac{1}{T_c}$, which are defined as $\mathbf{s}^{(u)} = \left[s_1^{(u)}, s_2^{(u)}, .., s_q^{(u)}, ..., s_S^{(u)}\right]^T$ and $\mathbf{h}_n^{(u)} = \left[h_n^{(u)}(1), h_n^{(u)}(2), .., h_n^{(u)}(w), ..., h_n^{(u)}(W)\right]^T$, where we have $u = 1, ..., U,\ q = 1, ..., S,\ w = 1, ..., W$ and $n = 1, ..., N$. The discretised composite received signal can be expressed as

$$\mathbf{y} = \mathbf{J}\mathbf{m} + \mathbf{n}, \quad (5)$$

where we have $\mathbf{y} = [y_1, y_2, ..., y_{NS+W-1}]^T$ and $\mathbf{n} = [n_1, n_2, ..., n_{NS+W-1}]^T$ with $\mathbf{n}$ representing the noise sequence, which has a covariance matrix of $\mathbf{R}_n = E[nn^H]$. In what follows we will discuss the operation of the iterative correlation and MMSE receivers.

1) Correlation Detector: The correlation detector is constituted by two filtering stages. The pre-whitening filter [13] is followed by the matched filter, as depicted in Figure. 1. The Cholesky decomposition of the noise covariance matrix $\mathbf{R}_n$ is given by

$$\mathbf{R}_n = \mathbf{L}\mathbf{L}^{\mathbf{H}}, \quad (6)$$

where $\mathbf{L}$ is a lower triangular matrix having real-valued elements on its main diagonal. The z-domain transfer function of the pre-whitening filter is $\mathbf{L}^{-1}$ [14]. The output of the pre-whitening filter can be expressed as

$$\mathbf{y}' = \mathbf{L}^{-1}\mathbf{y} = \mathbf{L}^{-1}\mathbf{J}\mathbf{m} + \mathbf{L}^{-1}\mathbf{n}. \quad (7)$$

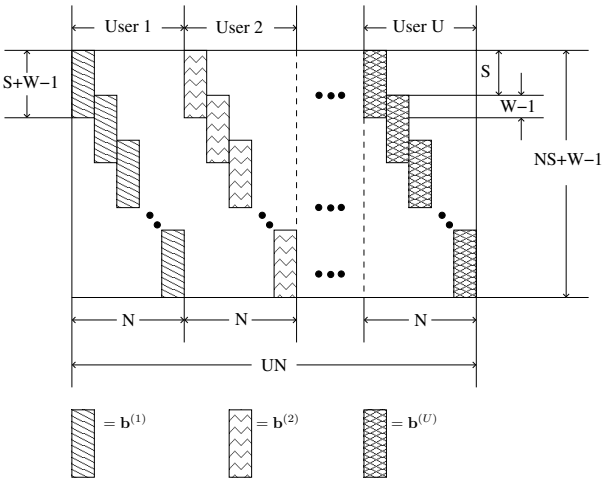

Fig. 3. Stylized structure of the system matrix $\mathbf{J}$, where $\mathbf{b}^{(1)}$,$\mathbf{b}^{(2)}$ and $\mathbf{b}^{(U)}$ are column vectors representing the combined impulse responses of users 1, 2, and U, respectively as seen in Equation (3) © Hanzo *et. al.* [13].

The discrete transfer function $\mathbf{T_{Mf}}$ of the matched filter may be formulated as [15]:

$$\mathbf{T_{Mf}} = (\mathbf{L^{-1}J})^{\mathbf{H}} = \mathbf{J^H}(\mathbf{L^{-1}})^{\mathbf{H}}. \quad (8)$$

Finally, combining Equations (7) and (8) provides joint estimates of the data symbols for the correlation detector expressed as:

$$\hat{\mathbf{m}}_{\mathbf{Corr}} = \mathbf{y}'' = \mathbf{T_{MF}}\mathbf{y}' = \mathbf{J^H}\mathbf{R_n^{-1}}\mathbf{y}. \quad (9)$$

Equation (9) can be expanded into the Multiple Access Interference (MAI) and InterSymbol Interference (ISI) as follows:

$$\hat{\mathbf{m}}_{\mathbf{Corr}} = \underbrace{diag(\mathbf{J^H}\mathbf{R_n^{-1}}\mathbf{J})\mathbf{m}}_{symbols} + \underbrace{\overline{diag}(\mathbf{J^H}\mathbf{R_n^{-1}}\mathbf{J})\mathbf{m}}_{ISI,MAI} + \underbrace{\mathbf{J^H}\mathbf{R_n^{-1}}\mathbf{n}}_{noise}, \quad (10)$$

It becomes clear from Equations (9) and (10) that the correlation detector is inefficient in terms of mitigating the MAI and ISI imposed in a multiuser and multipath scenario.

2) MMSE Detector: The MMSE detector minimises the simple quadratic form [15] $Q(\hat{\mathbf{m}}) = E\left[(\mathbf{m} - \hat{\mathbf{m}})^H(\mathbf{m} - \hat{\mathbf{m}})\right]$, where $\hat{\mathbf{m}}$ is the estimate of the data $\mathbf{m}$. Upon invoking the well-known Orthogonality Principle of [16]

$$E\left[(\mathbf{m} - \hat{\mathbf{m}})\mathbf{y}^H\right] = 0, \quad (11)$$

and substituting $\hat{\mathbf{m}} = \mathbf{P}\mathbf{y}$ in Equation (11) and then solving for $\mathbf{P}$, we arrive at

$$\mathbf{P} = \mathbf{R}_{my}\mathbf{R}_y^{-1}, \quad (12)$$

where $\mathbf{R}_{my} = E\left[\mathbf{m}\mathbf{y}^H\right]$ and $\mathbf{R}_y = E\left[\mathbf{y}\mathbf{y}^H\right]$ represent the corresponding covariance matrices. Substituting Equation (5) into $\mathbf{R}_{my} = E\left[\mathbf{m}\mathbf{y}^H\right]$ and $\mathbf{R}_y = E\left[\mathbf{y}\mathbf{y}^H\right]$, we arrive at

$$\mathbf{R}_{my} = \mathbf{R}_m\mathbf{J}^H, \quad (13)$$

$$\mathbf{R}_y = \mathbf{J}\mathbf{R}_m\mathbf{J}^H + \mathbf{R}_n, \quad (14)$$

where $\mathbf{R}_m = E\left[\mathbf{m}\mathbf{m}^H\right]$ is the covariance matrix of the data. Substituting Equations (13) and (14) in Equation (12) we obtain

$$\begin{aligned}\mathbf{P} &= \mathbf{R}_m\mathbf{J}^H(\mathbf{J}\mathbf{R}_m\mathbf{J}^H + \mathbf{R}_n)^{-1} \\ &= (\mathbf{J}^H\mathbf{R}_n^{-1}\mathbf{J} + \mathbf{R}_m^{-1})^{-1}\mathbf{J}^H\mathbf{R}_n^{-1}. \end{aligned} \quad (15)$$

Hence, the MMSE detector's estimated bits $\hat{\mathbf{m}}_{MMSE}$ can be expressed as

$$\hat{\mathbf{m}}_{MMSE} = (\mathbf{J}^H\mathbf{R}_n^{-1}\mathbf{J} + \mathbf{R}_m^{-1})^{-1}\mathbf{J}^H\mathbf{R}_n^{-1}\mathbf{y}. \quad (16)$$

Substituting Equation (5) into Equation (16) and partitioning it for the desired symbols, the MAI, ISI and noise are formulated as

$$\begin{aligned}\hat{\mathbf{m}}_{MMSE} &= \left[(\mathbf{J}^H\mathbf{R}_n^{-1}\mathbf{J} + \mathbf{R}_m^{-1})^{-1}\mathbf{J}^H\mathbf{R}_n^{-1}\right]\mathbf{J}\mathbf{m} + \\ &\quad (\mathbf{J}^H\mathbf{R}_n^{-1}\mathbf{J} + \mathbf{R}_m^{-1})^{-1}\mathbf{J}^H\mathbf{R}_n^{-1}\mathbf{n} \\ &= \underbrace{diag\Big(\left[\mathbf{I}_{KN} + (\mathbf{R}_m\mathbf{J}^H\mathbf{R}_n^{-1}\mathbf{J})^{-1}\right]^{-1}\Big)\mathbf{m}}_{symbols} \\ &+ \underbrace{\overline{diag}\Big(\left[\mathbf{I}_{KN} + (\mathbf{R}_m\mathbf{J}^H\mathbf{R}_n^{-1}\mathbf{J})^{-1}\right]^{-1}\Big)\mathbf{m}}_{ISI,MAI} \\ &+ \underbrace{(\mathbf{J}^H\mathbf{R}_n^{-1}\mathbf{J} + \mathbf{R}_m^{-1})^{-1}\mathbf{J}^H\mathbf{R}_n^{-1}\mathbf{n}}_{noise}. \end{aligned} \quad (17)$$

From Equations (16) and (17), it can be seen that unlike the Corr detector, the MMSE detector attempts to achieve a balance between eliminating the different types of data impairments including the noise, MAI and ISI in order to minimize the mean squared estimation error in the simple quadratic form [15] $Q(\hat{\mathbf{m}}) = E\left[(\mathbf{m} - \hat{\mathbf{m}})^H(\mathbf{m} - \hat{\mathbf{m}})\right]$, while the Corr detector simply estimates Equation (9) and hence fails to balance MAI and ISI produced by the mulituser and multipath envoirment. Explicitly, MMSE detection has a superior ability to mitigate the effects of MAI and ISI imposed in a multipath and multiuser scenario.

TABLE I
SYSTEM PARAMETERS

Spreading Factor	$N_s = 32$
No. of Users	$U = 20, 32$
Data Burst Length Per User	$N = 10$
$\Lambda\left[\frac{1}{nsec}\right]$(Cluster Arrival Rate)	0.0233
$\lambda\left[\frac{1}{nsec}\right]$(Ray Arrival Rate)	2.5
Γ(Cluster Decay Factor)	7.1
γ(Ray Decay Factor)	4.2
Outer Channel Code	RSC(2,1,5)
Inner Code	Rate 1 Code (URC)
Detector I	Correlation
Detector II	MMSE

IV. RESULTS AND DISCUSSION

In this section we present our system performance results. The system considered in this section obeys the schematic of Figure 1 and employs the parameters outlined in Table I for transmission over the IEEE 802.15.3a channel model [4].

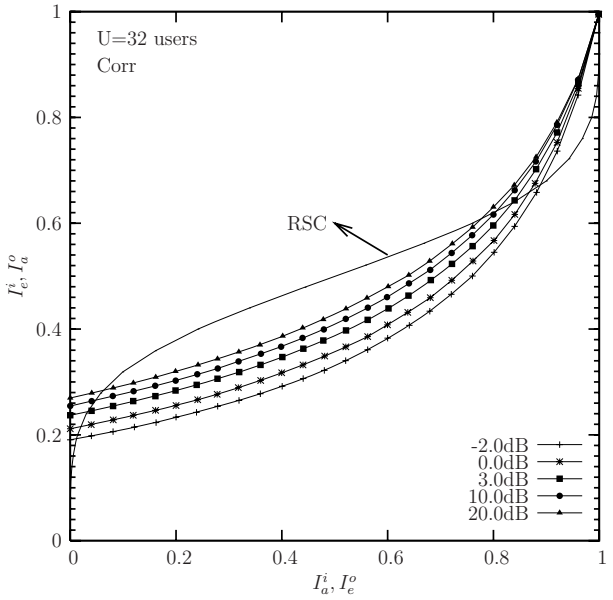

Fig. 4. EXIT charts and iterative decoding trajectory of the UWB DS-CDMA system using correlation detector and the parameters of Table 1.

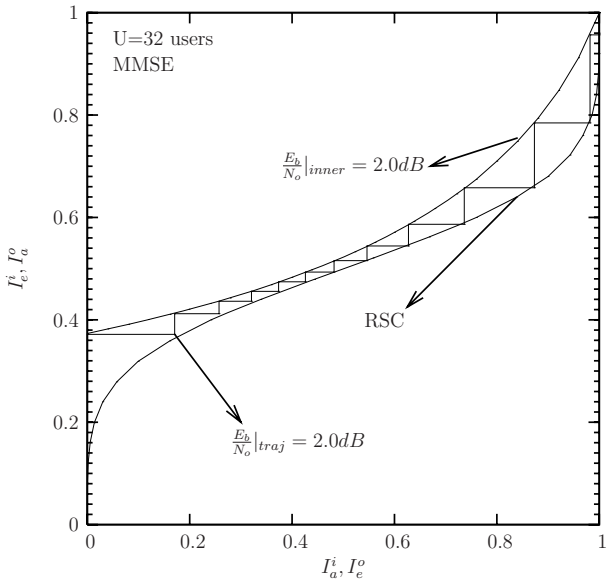

Fig. 5. EXIT charts and iterative decoding trajectory of the UWB DS-CDMA system using the MMSE detector and the parameters of Table 1.

The proposed system model employs a RSC code as the outer encoder and a URC as the inner encoder. We use a memory-two half-rate RSC code having a generator polynomial of $\left[1, \frac{1+D^2}{1+D+D^2}\right]$ and a memory-one recursive URC having a generator polynomial of $\left[\frac{1}{1+D}\right]$, as illustrated Figure 1. Figures 4 and 5 present the EXIT chart of the systems employing the Corr and MMSE detectors, respectively. These results were recorded for the fully-loaded system supporting $U = 32$ users with the aid of a spreading factor of $N_s = 32$ for transmission over the channel specified in Table I. Observe from Figure 5 that an open convergence tunnel is formed around $\frac{E_b}{N_o} = 2.0dB$. This implies that according to the predictions of the EXIT chart seen in Figure 5, the iterative decoding process is expected to converge at an $\frac{E_b}{N_o}$ value between 1dB and

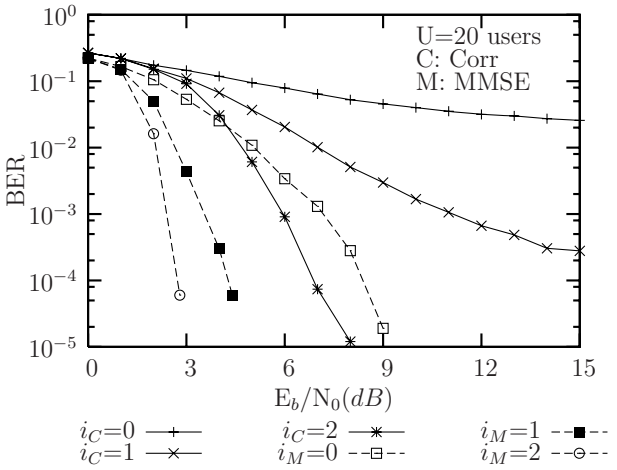

Fig. 6. BER Performance Comparison of Corr and MMSE detectors using an interleaver length $I = 100,000$ bits for a variable number of iterations and using the system parameters of Table 1.

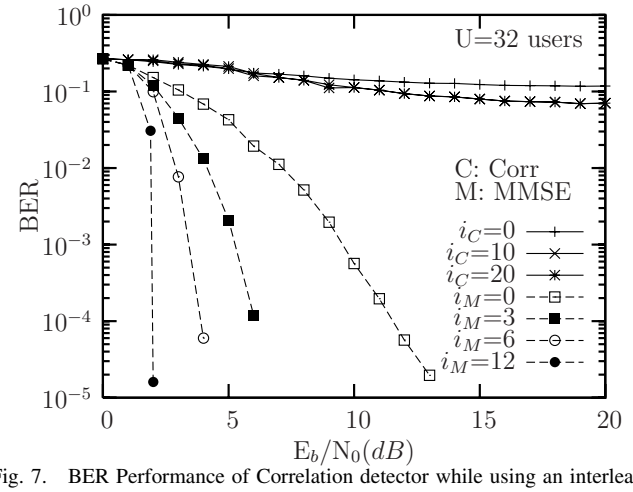

Fig. 7. BER Performance of Correlation detector while using an interleaver length $I = 100,000$ bits for a variable number of iterations, 32 users and using the system parameters outlined in Table 1.

2dB. The EXIT chart based iterative detection convergence predictions can be verified by the simulation-based iterative decoding trajectory of Figure 5, where the trajectory was recorded at $\frac{E_b}{N_o} = 2.0dB$, while using an interleaver length of $I = 100,000$ bits. By contrast, the EXIT curve of Figure 4 recorded for the Corr detector shows no open convergence tunnel even when we have $\frac{E_b}{N_o} = 20.0dB$. The reason for this is that the Corr detector is incapable of mitigating the MAI and ISI, as mentioned in Section III. Figure 6 shows the BER curves recorded for the Corr and MMSE detectors, when supporting $U = 20$ users with the aid of a spreading factor of $N_s = 32$. It is clear from Figure 6 that the MMSE detector has a superior performance from the very first iteration onwards. Finally, Figure 7 potrays the BER curves recorded for the system employing the Corr and MMSE detectors, respectively, the fully-loaded system supporting $U = 32$ users with the aid of a spreading factor of $N_s = 32$, while employing the system parameters outlined in Table I. As predicted by the EXIT charts of Figures 4 and 5 the MMSE detector outperforms the Corr detector also in terms of the BER curves of Figure 7.

V. Conclusion and Future Work

In this contribution we presented the performance study of a DS-CDMA UWB system communicating over the IEEE 802.15.3a UWB channel.The system used a serially concatenated and iteratively decoded convolutional code and URC combined with a MMSE or Correlation detector. Our future research will consider the performance versus complexity benefits of sophisticated detectors, such as sphere decoders. Furthermore, time hopping versus frequency hopping system studies will be conducted.

References

[1] L. Yang and G. B. Giannakis, "Ultra-wideband communications: an idea whose time has come," *IEEE Signal Processing Magazine*, vol. 21, pp. 26–54, Nov. 2004.

[2] Federal Communications Commission, "Revision of part 15 of the commission's rules regarding ultra-wideband transmission systems, first report and order," pp. ET Docket 98–153, 2002.

[3] M. Hamalainen, V. Hovinen, R. Tesi, J. H. J. Iinatti, and M. Latva-aho, "On the UWB system coexistence with GSM900, UMTS/WCDMA, and GPS," *IEEE Journal on Selected Areas in Communications*, vol. 20, pp. 1712–1721, Dec. 2002.

[4] A. F. Molisch, J. R. Foerster, and M. Pendergrass, "Channel models for ultrawideband personal area networks," *IEEE [see also IEEE Personal Communications] Wireless Communications*, vol. 10, pp. 14–21, Dec. 2003.

[5] T. K. L. Hanzo, W. Webb, *Single and Multicarrier Quadrature Amplitude Modulation*. John-Wiley IEEE Press, 2003.

[6] Stephan ten Brink, "Designing Iterative Decoding Schemes with the Extrinsic Information Transfer Chart," *AEÜ International Journal of Electronics and Communications*, vol. 54, pp. 389–398, Nov 2000.

[7] D. Divsalar, S. Dolinar, F. Pollara, "Serial concatenated trellis coded modulation with rate-1 inner code," in *IEEE Global Telecommunications Conference (GLOBECOM)*, vol. 2, (San Francisco, CA), pp. 777–782, 2000.

[8] S. ten Brink, "Convergence behavior of iteratively decoded parallel concatenated codes," *IEEE Transactions on Communications*, vol. 49, pp. 1727–1737, Oct. 2001.

[9] B. L. Y. L. Hanzo, T. H. Liew, *Turbo coding, turbo equalization and space-time coding: for transmission over fading channels*. Wiley: IEEE Press, 2002.

[10] S. Hara and R. Prasad, "Overview of multicarrier CDMA," *IEEE Communications Magazine*, vol. 35, pp. 126–133, Dec. 1997.

[11] K. Hao and J. A. Gubner, "The distribution of sums of path gains in the IEEE 802.15.3a UWB channel model," *IEEE Transactions on Wireless Communications*, vol. 6, pp. 811–816, Mar. 2007.

[12] A. Saleh and R. Valenzuela, "A statistical model for indoor multipath propagation," *IEEE Journal on Selected Areas in Communications*, vol. 5, pp. 128–137, Feb. 1987.

[13] L. Hanzo, L.-L. Yang, E.-L. Kuan, and K. Yen, *Single and Multi-Carrier DS-CDMA: Multi-user Detection, Space-Time Spreading, Synchronisation, Networking and Standards*. Chichester, England: John Wiley and Sons Ltd and IEEE Press, NY, USA, 2003.

[14] R. N. McDonough and A. D. Whalen, *Detection of Signals in Noise*. Academic Press, 1995.

[15] A. Klein, G. K. Kaleh, and P. W. Baier, "Zero forcing and minimum mean-square-error equalization formultiuser detection in code-division multiple-access channels," *IEEE Transactions on Vehicular Technology*, vol. 45, pp. 276–287, May 1996.

[16] D. F. Mix, *Random Signal Processing*. Prentice Hall, 1995.